

## RECENT CHARM RESULTS FROM FERMILAB EXPERIMENT E791

A.J. SCHWARTZ

*Department of Physics, University of Cincinnati,  
Cincinnati, Ohio 45221 (USA)*

Fermilab experiment E791 studied weak decays of  $D^+$ ,  $D_s^+$ , and  $D^0$  mesons produced in collisions of 500 GeV/c negative pions with Pt and C targets. The experiment collected over 200 000 fully reconstructed charm decays. Four recent results are discussed here: (a) measurement of the form factor ratios  $V/A_1$ ,  $A_2/A_1$ , and  $A_3/A_1$  in  $D^+ \rightarrow \bar{K}^{*0} \ell^+ \nu_\ell$  and  $D_s^+ \rightarrow \phi \ell^+ \nu_\ell$  decays; (b) measurement of the difference in decay widths  $\Delta\Gamma$  between the two  $D^0/\bar{D}^0$  mass eigenstates; (c) search for rare and forbidden  $D$  decays to dilepton final states; and (d) search for a ‘‘Pentaquark,’’ a bound state of  $\bar{c}suud$ .

**1 Introduction**

Fermilab E791 is a charm hadroproduction experiment studying the weak decays of charmed mesons and baryons. The experiment took data from September, 1991 to January, 1992, recording over  $2 \times 10^{10}$  interactions and reconstructing over 200 000 charm decays. This large sample has led to numerous published results.<sup>1</sup> Four recent results are discussed here: (a) measurement of the form factor ratios  $V/A_1$ ,  $A_2/A_1$ , and  $A_3/A_1$  in  $D^+ \rightarrow \bar{K}^{*0} \ell^+ \nu_\ell$  and  $D_s^+ \rightarrow \phi \ell^+ \nu_\ell$  decays;<sup>2</sup> (b) measurement of the difference in decay widths  $\Delta\Gamma$  between the two  $D^0/\bar{D}^0$  mass eigenstates;<sup>3</sup> (c) search for rare and forbidden  $D$  decays;<sup>4</sup> and (d) search for a ‘‘Pentaquark,’’ a bound state of  $\bar{c}suud$ .<sup>5,6</sup>

The E791 collaboration comprises approximately 70 physicists from 17 institutions.<sup>a</sup> The experiment produced charmed mesons and baryons using a  $\pi^-$  beam of momentum 500 GeV/c incident on five thin target foils (one platinum, four carbon). The foils were separated along the beamline by approximately 1.5 cm such that most charm decays occurred in air rather than in solid material. Immediately downstream of the target was a silicon strip vertex detector consisting of 17 planes of silicon strips oriented along the  $x$ ,  $y$ ,  $u$  and  $v$  directions, where  $u$  and  $v$  point  $\pm 20^\circ$  from the vertical direction ( $y$ ). Following the vertex detector was a spectrometer consisting of two large-aperture dipole magnets providing  $p_T$  kicks of 212 MeV/c and 320 MeV/c, and 37 planes of wire drift chambers and proportional chambers. Downstream of the second magnet were two threshold Čerenkov counters used to discriminate among pions, kaons, and protons. Following the Čerenkov counters was a Pb/liquid-scintillator calorimeter used to measure the energy of electrons and photons, and an Fe/plastic-scintillator calorimeter used to measure the energy of hadrons. Downstream of the calorimeters was approximately 1.0 m of iron to range out any remaining hadrons, and following the iron were two stations of plastic scintillator – one  $x$ -measuring and one  $y$ -measuring – to identify muons. The experiment used a loose transverse energy trigger ( $E_T \gtrsim 3$  GeV) that was almost fully efficient for charm decays.

After events were reconstructed, those with evidence of a decay vertex separated from the interaction vertex were retained for further analysis. The analyses presented here selected events using numerous kinematic and quality criteria; the most important of these are listed in Table 1.

<sup>a</sup> C.B.P.F. (Brazil), Tel Aviv (Israel), CINVESTAV (Mexico), Puebla (Mexico), U.C. Santa Cruz, University of Cincinnati, Fermilab, Illinois Institute of Technology, Kansas State, University of Massachusetts, University of Mississippi, Princeton, University of South Carolina, Stanford, Tufts, University of Wisconsin, and Yale.

Table 1: Kinematic and quality criteria used to select events.

Cut	Typical value
SDZ = $(z_{\text{sec}} - z_{\text{prim}}) / \sqrt{\sigma_{\text{sec}}^2 + \sigma_{\text{prim}}^2}$	12 ( $D^0, D_s^+$ ), 20 ( $D^+$ )
$p_T$ (transverse to $D$ line-of-flight)	< 250 MeV/c
$\Delta_z(\text{target}) = (z_{\text{sec}} - z_{\text{targ. edge}}) / \sigma_{\text{sec}}$	5.0 <
DIP = $D$ impact parameter w/r/t primary vertex	< 40 $\mu\text{m}$
$\chi_{\text{track}}^2 / (\text{d.o.f.})$	< 5.0
Lifetime = $(z_{\text{sec}} - z_{\text{prim}}) \cdot m_D / p$	< 3.0 ps ( $D^0, D_s^+$ ), < 5.0 ps ( $D^+$ )

An especially effective criterion for enhancing signal over background was ‘‘SDZ,’’ the longitudinal distance between the production and decay vertices divided by the total measurement error in this quantity.

## 2 $D^+$ and $D_s^+$ Form Factors

Semileptonic decays such as  $D^+ \rightarrow \bar{K}^{*0} \ell^+ \nu_\ell$  and  $D_s^+ \rightarrow \phi \ell^+ \nu_\ell$  proceed via spectator diagrams. As such, all hadronic effects are parametrized by four Lorentz-invariant form factors:  $A_1(q^2)$ ,  $A_2(q^2)$ ,  $A_3(q^2)$ , and  $V(q^2)$ . Unfortunately, the limited size of current data samples precludes measurement of the  $q^2$  dependence, and we assume this dependence to be given by a nearest pole dominance model:  $F(q^2) = F(0)/(1 - q^2/m_{\text{pole}}^2)$ , where  $m_{\text{pole}} = 2.1 \text{ GeV}/c^2$  for the vector form factor  $V$  and  $2.5 \text{ GeV}/c^2$  for the axial-vector form factors  $A$ . Because  $A_1(q^2)$  appears in every term in the differential decay rate, we factor out  $A_1(0)$  and measure the ratios  $r_V \equiv V(0)/A_1(0)$ ,  $r_2 \equiv A_2(0)/A_1(0)$ , and  $r_3 \equiv A_3(0)/A_1(0)$ . These ratios are insensitive to the total decay rate and to the weak mixing matrix element  $V_{cs}$ .

To select  $D^+ \rightarrow \bar{K}^{*0} \ell^+ \nu_\ell$  and  $D_s^+ \rightarrow \phi \ell^+ \nu_\ell$  decays, we identify 3-track vertices in which one track is identified as a kaon and one track as a lepton. We cut on the ‘‘transverse’’ mass  $m_T$ , where  $m_T^2 \equiv (E_{K^*/\phi} + E_\ell + p_T)^2 - (\mathbf{p}_{K^*/\phi} + \mathbf{p}_\ell + \mathbf{p}_T)^2$ . In this expression,  $\mathbf{p}_T$  is the momentum of the neutrino transverse to the direction of the  $D$  as inferred by momentum balance. The  $m_T$  distribution of semileptonic decays forms a Jacobian peak with an endpoint at  $m_D$ , and thus we require that  $m_T$  lie in the range 1.6–2.0  $\text{GeV}/c^2$  (1.7–2.1  $\text{GeV}/c^2$ ) for the  $D^+$  ( $D_s^+$ ) sample. We also require that either  $m_{K\pi} \approx m_{K^*}$  or  $m_{KK} \approx m_\phi$ . The resulting samples contain very little background, and we do a maximum likelihood fit for the form factors using a likelihood function based on three angles:  $\theta_V$ , the polar angle in the  $\bar{K}^{*0}$  ( $\phi$ ) rest frame between the  $\pi^+$  ( $K^+$ ) and the  $D^+$  ( $D_s^+$ );  $\theta_\ell$ , the polar angle in the  $W^+$  rest frame between the  $\nu_\ell$  and the  $D^+$  ( $D_s^+$ ); and  $\chi$ , the azimuthal angle in the  $D^+$  ( $D_s^+$ ) rest frame between the  $\bar{K}^{*0}$  ( $\phi$ ) and  $W^+$  decay planes. The results of the fit to the  $\bar{K}^{*0}$  data for the  $e + \mu$  samples combined are:  $r_V = 1.87 \pm 0.08 \pm 0.07$  and  $r_2 = 0.73 \pm 0.06 \pm 0.08$ . We measure  $r_3 = 0.04 \pm 0.33 \pm 0.29$  from the  $\mu$  sample alone. The results for  $D_s^+ \rightarrow \phi \ell^+ \nu_\ell$  are:  $r_V = 2.27 \pm 0.35 \pm 0.22$  and  $r_2 = 1.57 \pm 0.25 \pm 0.19$ . These results are compared with theoretical predictions in Table 2; the errors in the measurements are smaller than the spread in theoretical predictions.

## 3 $D^0$ - $\bar{D}^0$ Mixing and $\Delta\Gamma$

E791 has published a limit on the  $D^0$ - $\bar{D}^0$  mixing rate using semileptonic  $D^0 \rightarrow K^- \ell^+ \nu_\ell$  decays<sup>19</sup> and hadronic  $D^0 \rightarrow K^- \pi^+$  and  $D^0 \rightarrow K^- \pi^+ \pi^- \pi^+$  decays.<sup>20</sup> The flavor of the  $D^0$  or  $\bar{D}^0$  when produced is determined by combining the  $D^0/\bar{D}^0$  with a low momentum pion to reconstruct

Table 2: Theoretical predictions for  $r_V$  and  $r_2$ . Some values are extrapolations from  $q^2 = q_{\text{max}}^2$  to  $q^2 = 0$ .

Group	$r_V$	$r_2$
<b>E791 <math>D^+ \rightarrow \bar{K}^{*0} \ell^+ \nu_\ell</math></b>	<b><math>1.87 \pm 0.11</math></b>	<b><math>0.73 \pm 0.10</math></b>
ISGW2 <sup>7</sup>	2.0	1.3
WSG <sup>8</sup>	1.4	1.3
KS <sup>9</sup>	1.0	1.0
AW/GS <sup>10</sup>	2.0	0.8
Stech <sup>11</sup>	1.55	1.06
BKS <sup>12</sup>	$1.99 \pm 0.22 \pm 0.33$	$0.7 \pm 0.16 \pm 0.17$
LMMS <sup>13</sup>	$1.6 \pm 0.2$	$0.4 \pm 0.4$
ELC <sup>14</sup>	$1.3 \pm 0.2$	$0.6 \pm 0.3$
APE <sup>15</sup>	$1.6 \pm 0.3$	$0.7 \pm 0.4$
UKQCD <sup>16</sup>	$1.4^{+0.5}_{-0.2}$	$0.9 \pm 0.2$
BBD <sup>17</sup>	$2.2 \pm 0.2$	$1.2 \pm 0.2$
LANL <sup>18</sup>	$1.78 \pm 0.07$	$0.68 \pm 0.11$
<b>E791 <math>D_s^+ \rightarrow \phi \ell^+ \nu_\ell</math></b>	<b><math>2.27 \pm 0.41</math></b>	<b><math>1.57 \pm 0.31</math></b>
ISGW2 <sup>7</sup>	2.1	1.3
BKS <sup>12</sup>	$2.00 \pm 0.19^{+0.20}_{-0.25}$	$0.78 \pm 0.08^{+0.17}_{-0.13}$
LMMS <sup>13</sup>	$1.65 \pm 0.21$	$0.33 \pm 0.33$

a  $D^{*+} \rightarrow D^0 \pi^+$  or  $D^{*-} \rightarrow \bar{D}^0 \pi^-$  decay. The semileptonic decays yield a 90% C.L. limit  $r_{\text{mix}} < 0.50\%$  [where  $r_{\text{mix}} \equiv \Gamma(D^0 \rightarrow \bar{D}^0 \rightarrow \bar{f})/\Gamma(D^0 \rightarrow f)$ ], while the hadronic decays yield a 90% C.L. limit  $r_{\text{mix}} < 0.85\%$ . The latter limit assumes no  $CP$  violation in the mixing and no  $CP$  violation in a doubly-Cabibbo-suppressed (DCS) amplitude which also contributes to the rate. However,  $CP$  violation is allowed in the *interference* between the mixing and DCS amplitudes. Since the DCS amplitude is in fact substantially larger than that expected from mixing, the presence of “wrong-sign” decays in the hadronic data – while a signature for mixing – is more easily interpreted as evidence for DCS decays. If we assume no mixing, then the numbers of wrong-sign decays observed in our data, corrected for acceptance, imply ratios of DCS decays to Cabibbo-favored decays of  $r_{\text{DCS}}^{K\pi} = (0.68^{+0.34}_{-0.33} \pm 0.07)\%$  and  $r_{\text{DCS}}^{K\pi\pi\pi} = (0.25^{+0.36}_{-0.34} \pm 0.03)\%$ .

Since  $r_{\text{mix}} = (1/2) [(\Delta m/\Gamma)^2 + (\Delta\Gamma/2\Gamma)^2]$ , where  $\Delta m$  and  $\Delta\Gamma$  are the differences between the masses and decay widths of the  $D^0/\bar{D}^0$  mass eigenstates, the upper limit for  $r_{\text{mix}}$  implies an upper limit for the difference in widths:  $|\Delta\Gamma| < 0.48 \text{ ps}^{-1}$ . E791 has made a direct measurement of  $\Delta\Gamma$  using  $D^0 \rightarrow K^- K^+$  and  $D^0 \rightarrow K^- \pi^+$  decays. Since the former results in a  $CP$ -even eigenstate, only the  $CP$ -even component  $D_1^0$  contributes and the lifetime distribution is proportional to  $e^{-\Gamma_1 t}$ . The  $K^- \pi^+$  final state, however, is a  $CP$  admixture and the lifetime distribution is proportional to  $\exp[-(\Gamma_1 + \Gamma_2)t/2] \cosh(\Delta\Gamma t/2)$ .<sup>21</sup> Over the range of lifetimes for which the experiment has sensitivity,  $\cosh(\Delta\Gamma t/2) \approx 1$  and thus:  $\Gamma_{KK} - \Gamma_{K\pi} = \Gamma_1 - (\Gamma_1 + \Gamma_2)/2 = (\Gamma_1 - \Gamma_2)/2 = \Delta\Gamma/2$ .

Our samples of  $D^0 \rightarrow K^- K^+$  and  $D^0 \rightarrow K^- \pi^+$  are shown in Fig. 1a. We bin these events by *reduced* proper lifetime, which is the distance traveled by the  $D^0$  candidate beyond that required to survive our selection criteria, multiplied by mass and divided by momentum. For each bin of reduced lifetime we fit the mass distribution for the number of signal events. Plotting this number (corrected for acceptance) as a function of reduced lifetime gives the distributions shown in Fig. 1b. Fitting these distributions to exponential functions yields  $\Gamma_{KK} = 2.441 \pm 0.068 \text{ ps}^{-1}$ ,  $\Gamma_{K\pi} = 2.420 \pm 0.019 \text{ ps}^{-1}$ , and thus  $\Delta\Gamma = 0.04 \pm 0.14 \pm 0.05 \text{ ps}^{-1}$ . This implies  $-0.20 < \Delta\Gamma < 0.28 \text{ ps}^{-1}$  at 90% C.L., which is more stringent than the constraint resulting from  $r_{\text{mix}}$ .

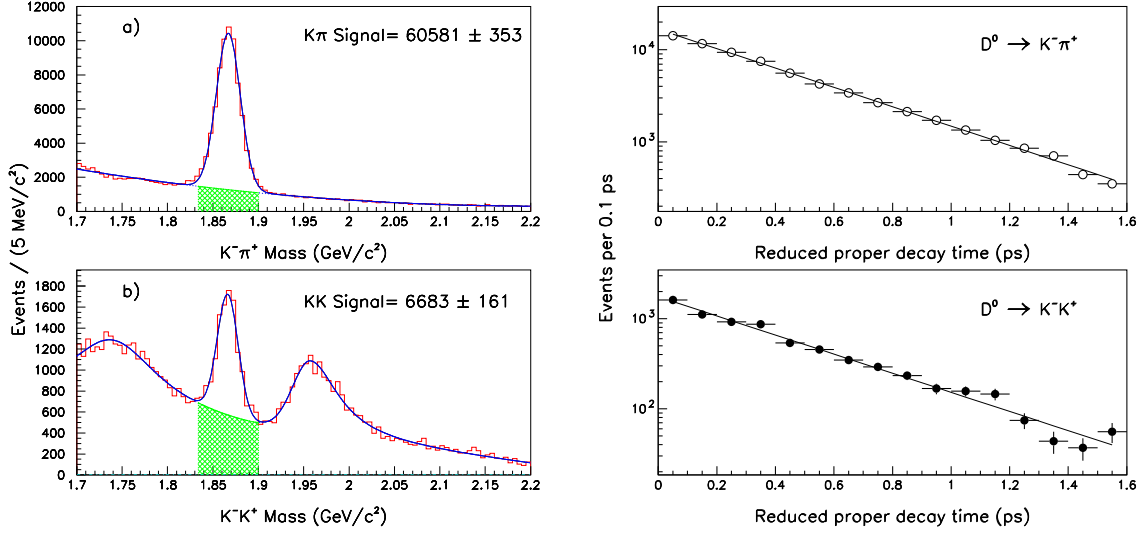


Figure 1:  $D^0 \rightarrow K^- \pi^+$  and  $D^0 \rightarrow K^- K^+$  mass distributions (left), and reduced proper lifetime distributions (right). The right-most peak in the lower left plot is due to misidentified  $D^0 \rightarrow K^- \pi^+$  decays.

#### 4 Rare and Forbidden $D$ Decays

E791 has searched for rare and forbidden dilepton decays of the  $D^+$ ,  $D_s^+$ , and  $D^0$ . The decay modes can be classified as follows:

1. flavor-changing neutral current decays  $D^0 \rightarrow \ell^+ \ell^-$  and  $D_{(d,s)}^+ \rightarrow h^+ \ell^+ \ell^-$ , in which  $h$  is a pion or kaon;
2. lepton-flavor violating decays  $D^0 \rightarrow \mu^\pm e^\mp$ ,  $D_{(d,s)}^+ \rightarrow h^+ \mu^\pm e^\mp$ , and  $D_{(d,s)}^+ \rightarrow h^- \mu^+ e^+$ , in which the leptons belong to different generations; and
3. lepton-number violating decays  $D_{(d,s)}^+ \rightarrow h^- \ell^+ \ell^+$ , in which the leptons belong to the same generation but have the same sign charge.

Decay modes belonging to (1) occur within the Standard Model via higher-order diagrams, but the branching fractions are estimated<sup>22</sup> to be only  $10^{-8}$  to  $10^{-6}$ . This is below the sensitivity of current experiments. Decay modes belonging to (2) and (3) do not conserve lepton number and thus are forbidden within the Standard Model. However, a number of theoretical extensions to the Standard Model predict lepton number violation,<sup>23</sup> and the observation of a signal in these modes would indicate new physics. We have searched for 24 different rare and forbidden decay modes and have found no evidence for them. We therefore present upper limits on their branching fractions. Eight of these modes have no previously reported limits, and fourteen are reported with substantial improvements over previously published results.

For this study we used a “blind” analysis technique. Before our selection criteria were finalized, all events having masses within a window  $\Delta M_S$  around the mass of the  $D^+$ ,  $D_s^+$ , or  $D^0$  were masked so that the presence or absence of potential signal candidates would not bias our choice of selection criteria. All criteria were then chosen by studying signal events generated by Monte Carlo simulation and background events obtained from the data. The background events were chosen from mass windows  $\Delta M_B$  above and below the signal window  $\Delta M_S$ . The criteria were chosen to maximize the ratio  $N_S/\sqrt{N_B}$ , where  $N_S$  and  $N_B$  are the numbers of signal and background events, respectively. Only after this procedure were events within the signal window unmasked. The signal windows  $\Delta M_S$  used for decay modes containing electrons are asymmetric around  $m_D$  to allow for the bremsstrahlung low-energy tail.

We normalize the sensitivity of our search to topologically similar Cabibbo-favored decays. For the  $D^+$  modes we use  $D^+ \rightarrow K^- \pi^+ \pi^+$ ; for the  $D_s^+$  modes we use  $D_s^+ \rightarrow \phi \pi^+$ ; and for the  $D^0$  we use  $D^0 \rightarrow K^- \pi^+$ . The upper limit on the branching fraction for decay mode  $X$  is:

$$B_X = \frac{N_X}{N_{\text{norm}}} \frac{\varepsilon_{\text{norm}}}{\varepsilon_X} \cdot B_{\text{norm}} , \quad (1)$$

where  $N_X$  is the upper limit on the mean number of signal events,  $N_{\text{norm}}$  is the number of normalization events, and  $\varepsilon_X$  and  $\varepsilon_{\text{norm}}$  are overall detection efficiencies. The geometric acceptances and reconstruction efficiencies are found from Monte Carlo simulation, and the particle identification efficiencies are measured from data.

The background consists of random combinations of tracks and vertices, and reflections from more copious hadronic  $D$  decays. The former is essentially flat in the reconstructed invariant mass, and we estimate this background by scaling the level from mass regions above and below the signal region  $\Delta M_S$ . The hadronic decay background in which a  $K$  is misidentified as a lepton is explicitly removed via a  $K\pi\pi$  or  $KK\pi$  invariant mass cut. The hadronic background in which a  $\pi$  is misidentified as a lepton cannot be removed in this manner, as the reflected mass and true mass are too close and such a cut would remove a substantial fraction of signal events. We thus estimate this background by multiplying the number of  $D^+ \rightarrow \pi^- \pi^+ \pi^+$ ,  $D_s^+ \rightarrow K^- \pi^+ \pi^+$ , or  $D^0 \rightarrow \pi^+ \pi^-$  decays falling within the signal region  $\Delta M_S$  by the rate for double particle misidentification  $\pi\pi \rightarrow \mu\mu$ ,  $\mu e$ , or  $ee$ . The misidentification rates were measured from data using  $D^+ \rightarrow K^- \pi^+ \pi^+$  decays misidentified as  $K^- \ell^+ \ell^+$ . Because the latter samples have substantial feedthrough background from the former (which is Cabibbo-favored), we do not attempt to establish a limit for  $D^+ \rightarrow K^- \ell^+ \ell^+$  decays. Rather, we use the observed signals to measure the lepton misidentification rates under the assumption that all  $K^- \ell^+ \ell^+$  decays observed arise from misidentified  $K^- \pi^+ \pi^+$ . Most of our final event samples are shown in Fig. 2, and all results are tabulated in Table 3.

## 5 Search for the Pentaquark $P_{\bar{c}s u u d}^0$

E791 has searched for a ‘‘Pentaquark’’  $P^0$ , which is a bound state of five quarks having flavor quantum numbers  $\bar{c}s u u d$ . This state was originally proposed by Lipkin<sup>25</sup> and Gignoux *et al.*<sup>26</sup> over ten years ago, but no experimental searches have been undertaken. The  $P^0$  is predicted to have a mass below the threshold for strong decay ( $m_{D_s} + m_p = 2.907 \text{ GeV}/c^2$ ) by 10–150  $\text{MeV}/c^2$ . The lifetime is expected to be similar to that of the shortest-lived charm meson, 0.4–0.5 ps. We have searched for  $P^0$  decays into  $\phi p \pi^-$  and  $K^{*0} K^- p$  final states.

The analysis proceeds by first selecting four-track vertices in which one track is identified as a proton and two opposite-sign tracks are identified as kaons. We require that either  $m_{KK} \approx m_\phi$  or  $m_{K\pi} \approx m_{K^*}$  and remove events in which either  $m_{p\pi} \approx m_\Lambda$  or the  $\phi$  or  $p$  momentum projects back to the production vertex. We normalize the sensitivity of the search to  $D_s^+ \rightarrow \phi \pi^+$  and  $D_s^+ \rightarrow \bar{K}^{*0} K^+$  decays; these are topologically similar to  $P^0 \rightarrow \phi p \pi^-$  and  $P^0 \rightarrow K^{*0} K^- p$  (except for the proton) and several systematic errors cancel. After all selection criteria are applied, we observe no excess of events above background in either decay channel. We thus obtain upper limits for the product of production cross section and branching fraction, relative to that for the  $D_s^+$ . The expression used is (here for  $\phi p \pi^-$ ):

$$\frac{\sigma_P \cdot B_{P \rightarrow \phi p \pi}}{\sigma_{D_s} \cdot B_{D_s \rightarrow \phi \pi}} = \frac{N_{P \rightarrow \phi p \pi}}{N_{D_s \rightarrow \phi \pi}} \frac{\varepsilon_{D_s \rightarrow \phi \pi}}{\varepsilon_{P \rightarrow \phi p \pi}} , \quad (2)$$

where  $N_{P \rightarrow \phi p \pi}$  is the upper limit on the mean number of  $P^0 \rightarrow \phi p \pi$  decays, and  $N_{D_s \rightarrow \phi \pi}$  is the number of events observed in the normalization channel. All numbers and the resulting limits

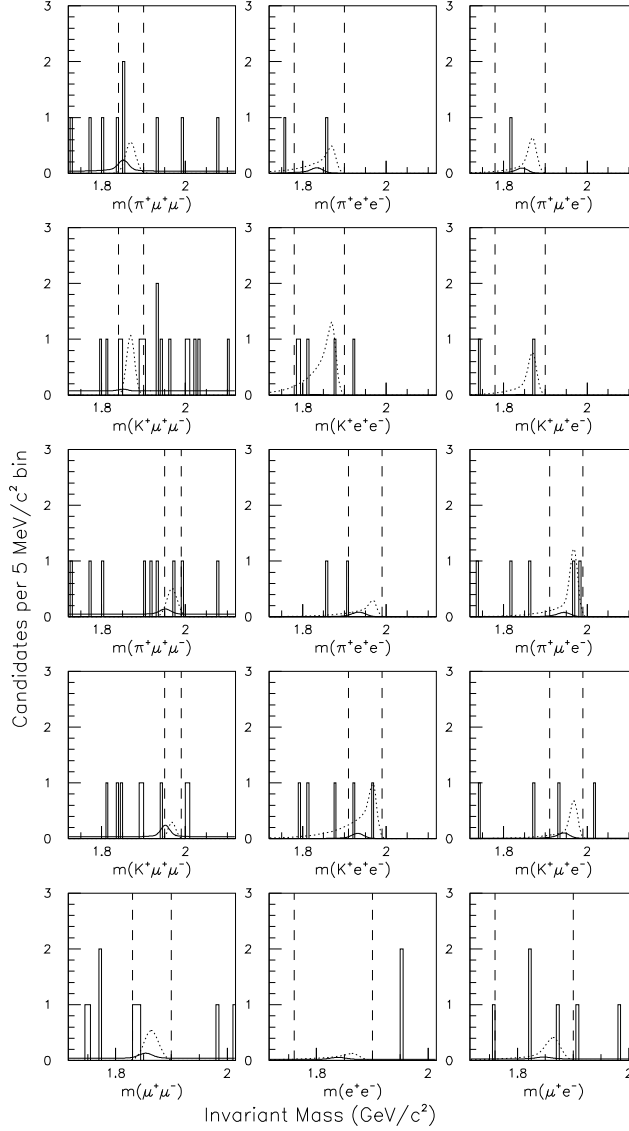


Figure 2: Final event samples for  $D^+$  (rows 1–2),  $D_s^+$  (rows 3–4), and  $D^0$  (row 5) decays. The dotted curves show signal shape for a number of events equal to the 90% C.L. limit. The solid curves show estimated background.

are listed in Table 4. When calculating acceptance, we assume the  $P^0$  lifetime to be 0.4 ps. The limits are given for two possible values of  $m_{P^0}$ ; the difference in the limits is due mainly to the difference in the numbers of events observed in the mass spectrum around these mass values. Our upper limits are 2–4% of that for the corresponding  $D_s^+$  decay, which is similar to the theoretical estimate ( $\sim 1\%$ ).

## 6 Summary

We have presented four recent results from Fermilab experiment E791: a measurement of the form factors governing  $D^+ \rightarrow \bar{K}^{*0} \ell^+ \nu_\ell$  and  $D^+ \rightarrow \phi \ell^+ \nu_\ell$  decays; a measurement of the difference in decay widths  $\Delta\Gamma$  between the two mass eigenstates of  $D^0/\bar{D}^0$ ; new limits on two dozen rare and forbidden dilepton decays of  $D^0$ ,  $D^+$ , and  $D_s^+$ ; and a limit on  $\sigma \cdot B$  for a ‘‘Pentaquark’’  $P^0$  relative to that for the  $D_s^+$ . Almost all measurements and limits are superior to previously

Table 3: 90% C.L. upper limits for dilepton decays of  $D^+/D_s^+/D^0$ . The right-most column lists previous results.

Mode	Background	Observed	UL ( $N$ )	UL( $B$ ) ( $\times 10^5$ )	PDG 98 <sup>24</sup> ( $\times 10^5$ )
$D^+ \rightarrow \pi^+ \mu^+ \mu^-$	2.67	2	3.35	< 1.5	< 1.8
$D^+ \rightarrow \pi^+ e^+ e^-$	0.90	1	3.53	< 5.2	< 6.6
$D^+ \rightarrow \pi^+ \mu^\pm e^\mp$	0.78	1	3.64	< 3.4	< 12
$D^+ \rightarrow \pi^- \mu^+ \mu^+$	1.53	1	2.92	< 1.7	< 8.7
$D^+ \rightarrow \pi^- e^+ e^+$	0.45	2	5.60	< 9.6	< 11
$D^+ \rightarrow \pi^- \mu^+ e^+$	0.39	1	4.05	< 5.0	< 11
$D^+ \rightarrow K^+ \mu^+ \mu^-$	2.40	3	5.07	< 4.4	< 9.7
$D^+ \rightarrow K^+ e^+ e^-$	0.09	4	8.72	< 20	< 20
$D^+ \rightarrow K^+ \mu^\pm e^\mp$	0.08	1	4.34	< 6.8	< 13
$D_s^+ \rightarrow K^+ \mu^+ \mu^-$	2.00	0	1.32	< 14	< 59
$D_s^+ \rightarrow K^+ e^+ e^-$	0.85	2	5.77	< 160	—
$D_s^+ \rightarrow K^+ \mu^\pm e^\mp$	1.10	1	3.57	< 63	—
$D_s^+ \rightarrow K^- \mu^+ \mu^+$	1.04	0	1.68	< 18	< 59
$D_s^+ \rightarrow K^- e^+ e^+$	0.39	0	2.22	< 63	—
$D_s^+ \rightarrow K^- \mu^+ e^+$	1.15	1	3.53	< 68	—
$D_s^+ \rightarrow \pi^+ \mu^+ \mu^-$	1.65	1	3.02	< 14	< 43
$D_s^+ \rightarrow \pi^+ e^+ e^-$	0.83	0	1.85	< 27	—
$D_s^+ \rightarrow \pi^+ \mu^\pm e^\mp$	0.72	2	6.01	< 61	—
$D_s^+ \rightarrow \pi^- \mu^+ \mu^+$	1.16	0	1.60	< 8.2	< 43
$D_s^+ \rightarrow \pi^- e^+ e^+$	0.42	1	4.44	< 69	—
$D_s^+ \rightarrow \pi^- \mu^+ e^+$	0.36	3	8.21	< 73	—
$D^0 \rightarrow \mu^+ \mu^-$	2.46	2	3.51	< 0.52	< 0.41
$D^0 \rightarrow e^+ e^-$	2.04	0	1.26	< 0.62	< 1.3
$D^0 \rightarrow \mu^\pm e^\mp$	2.88	2	3.09	< 0.81	< 1.9

Table 4: 90% C.L. upper limits on the product of cross section and branching fraction ( $\sigma \cdot B$ ) for  $P^0 \rightarrow \phi p \pi^-$  decays (left table) and  $P^0 \rightarrow K^{*0} K^- p$  decays (right table), relative to that for  $D_s^+ \rightarrow \phi \pi^+$  and  $D_s^+ \rightarrow \bar{K}^{*0} K^+$ .

	$P^0$ mass ( $\text{GeV}/c^2$ )	
	<b>2.79</b>	<b>2.87</b>
$UL(N_{P^0 \rightarrow \phi p \pi^-})$ :	3.1	7.5
$\varepsilon_P/\varepsilon_{D_s}$ :	0.47	0.64
$N_{D_s}$ :	293 $\pm$ 18	
Upper limit:	0.022	0.040

	$P^0$ mass ( $\text{GeV}/c^2$ )	
	<b>2.77</b>	<b>2.85</b>
$UL(N_{P^0 \rightarrow K^* K p})$ :	6.1	3.5
$\varepsilon_P/\varepsilon_{D_s}$ :	0.23	0.31
$N_{D_s}$ :	725 $\pm$ 88	
Upper limit:	0.036	0.016

published results. In the case of the  $P^0$  and eight of the rare and forbidden dilepton decays, our limits are the first such limits reported.

## References

1. See: <http://fnphyx-www.fnal.gov/experiments/e791/docs/publications>.
2. E. M. Aitala *et al.*, *Phys. Lett. B* **440**, 435 (1998); *Phys. Lett. B* **450**, 294 (1999).
3. E. M. Aitala *et al.*, *Phys. Rev. Lett.* **83**, 32 (1999).
4. E. M. Aitala *et al.*, FERMILAB Pub-99/183-E, to appear in *Phys. Lett. B*.
5. E. M. Aitala *et al.*, *Phys. Rev. Lett.* **81**, 44 (1998).
6. E. M. Aitala *et al.*, *Phys. Lett. B* **448**, 303 (1999).
7. D. Scora and N. Isgur, *Phys. Rev. D* **52**, 2783 (1995).
8. M. Wirbel, B. Stech, and M. Bauer, *Z. Phys. C* **29**, 637 (1985).
9. J. G. Körner and G. A. Schuler, *Phys. Lett. B* **226**, 185 (1989).
10. T. Altomari and L. Wolfenstein, *Phys. Rev. D* **37**, 681 (1988);  
F. J. Gilman and R. L. Singleton Jr., *Phys. Rev. D* **41**, 142 (1990).
11. B. Stech, *Z. Phys. C* **75**, 245 (1997).
12. C. W. Bernard *et al.*, *Phys. Rev. D* **47**, 998 (1993); *Phys. Rev. D* **45**, 869 (1992).
13. V. Lubicz *et al.*, *Phys. Lett. B* **274**, 415 (1992).
14. A. Abada *et al.*, *Nucl. Phys. B* **416**, 675 (1994).
15. C. R. Alton *et al.*, *Phys. Lett. B* **345**, 513 (1995).
16. K. C. Bowler *et al.*, *Phys. Rev. D* **51**, 4905 (1995).
17. P. Ball, V. M. Braun, and H. G. Dosch, *Phys. Rev. D* **44**, 3567 (1991).
18. T. Bhattacharya and R. Gupta, *Nucl. Phys. B* **47**, 481 (1996).
19. E. M. Aitala *et al.*, *Phys. Rev. Lett.* **77**, 2384 (1996).
20. E. M. Aitala *et al.*, *Phys. Rev. D* **57**, 13 (1998).
21. Here we have neglected the very small rate of (DCS)  $\bar{D}^0 \rightarrow K^- \pi^+$  decays.  
See: A. J. Schwartz, U. of Cincinnati Report UCTP-104-99.
22. A. J. Schwartz, *Mod. Phys. Lett. A* **8**, 967 (1993);  
P. Singer and D.-X. Zhang, *Phys. Rev. D* **55**, 1127 (1997).
23. See for example: S. Pakvasa, hep-ph/9705397 (1997); *Chin. J. Phys.* **32**, 1163 (1994).
24. C. Caso *et al.* (Particle Data Group), *Eur. Phys. J. C* **3**, 1 (1998).
25. H. J. Lipkin, *Phys. Lett. B* **195**, 484 (1987).
26. C. Gignoux *et al.*, *Phys. Lett. B* **193**, 323 (1987).